ANNUAL REVIEWS

Annual Review of Biomedical Engineering

Computer-Aided Design of Microfluidic Circuits

Elishai Ezra Tsur

Neuro-Biomorphic Engineering Lab (NBEL), Department of Mathematics and Computer Science, The Open University of Israel, Raanana 4353701, Israel; email: elishai@nbel-lab.com

Annu. Rev. Biomed. Eng. 2020. 22:285–307

The *Annual Review of Biomedical Engineering* is online at bioeng.annualreviews.org

https://doi.org/10.1146/annurev-bioeng-082219-033358

Keywords

microfluidics, continuous flow-based microfluidics, design automation, optimization algorithms, resistive microfluidic networks

Abstract

Microfluidic devices developed over the past decade feature greater intricacy, increased performance requirements, new materials, and innovative fabrication methods. Consequentially, new algorithmic and design approaches have been developed to introduce optimization and computer-aided design to microfluidic circuits: from conceptualization to specification, synthesis, realization, and refinement. The field includes the development of new description languages, optimization methods, benchmarks, and integrated design tools. Here, recent advancements are reviewed in the computer-aided design of flow-, droplet-, and paper-based microfluidics. A case study of the design of resistive microfluidic networks is discussed in detail. The review concludes with perspectives on the future of computer-aided microfluidics design, including the introduction of cloud computing, machine learning, new ideation processes, and hybrid optimization.

Contents

1. INTRODUCTION 286
2. COMPUTER-AIDED DESIGN 288
3. COMPUTER-AIDED DESIGN OF CONTINUOUS MICROFLUIDICS 291
   3.1. Description Languages 291
   3.2. Design for Optimization 292
   3.3. Standards and Benchmarks 294
   3.4. Design Tools 294
   3.5. Case Study: Computer-Aided Design of Resistive Microfluidic Networks 294
4. COMPUTER-AIDED DESIGN OF DROPLET-BASED MICROFLUIDICS 298
5. COMPUTER-AIDED DESIGN OF PAPER MICROFLUIDICS 299
6. PERSPECTIVES 300
   6.1. From Integrated Circuits to Microfluidics 301
   6.2. Hybrid Optimization and 3-D Fabrication 301
   6.3. Computer-Aided Design for Design Ideation 301
   6.4. Machine Learning 301
   6.5. Cloud Computing 302

1. INTRODUCTION

Microfluidics is a rapidly growing field with applications ranging from soft robotics (1) to quantum physics (2), single-cell sequencing (3), and point-of-care diagnostics (4, 5). Principally, microfluidics is the science of the precise manipulation of fluids at a micro- to pico-liter scales, and it can be broadly discriminated into (*a*) continuous (flow-based) microfluidics, in which fluids flow in closed mechanical channels and are controlled using integrated microvalves (6, 7) (**Figure 1*a***); (*b*) droplet-based microfluidics, in which drops of fluids are manipulated within immiscible phases (8) (**Figure 1*b***); (*c*) paper-based microfluidics, in which fluids are passively transported along hydrophobic physical barriers on hydrophilic paper (9) (**Figure 1*c***); and (*d*) digital microfluidics, in which fluids are manipulated as drops on a cell grid, with each cell having a controllable level of wetting characteristics (10) (**Figure 1*d***). For the purpose of this review, the first three categories are called pattern-based microfluidics as they require application-specific mechanical design.

New integrations among these different paradigms have created hybrid microfluidic technologies that have unique advantages; for example, paper-based digital microfluidics, in which conductive ink is printed onto photo paper to create electrodes and control lines, offers digital microfluidics capabilities with faster in-place fabrication, lower costs, and higher disposability (11). A particularly interesting emerging technology that has evolved from continuous microfluidics is programmable microfluidics, often implemented with fully programmable valve arrays (FPVAs) (12, 13) (**Figure 1*e***). An FPVA is a dense grid of switchable blocks, with which fluid can be manipulated in highly configurable and programmable patterns. An FPVA provides a standard microfluidic architecture that can be configured to flexibly support nearly any relevant application. Another hybrid microfluidic technology, termed co-synthesis, integrates digital and continuous microfluidics to offer real-time resource allocation for concurrent analyses (14).

The design process of pattern-based microfluidics initiates with system specifications and concludes with a topological graph that describes its mechanical architecture. Predominantly, topological descriptions are manually drawn with vector graphics editors. These computer-aided

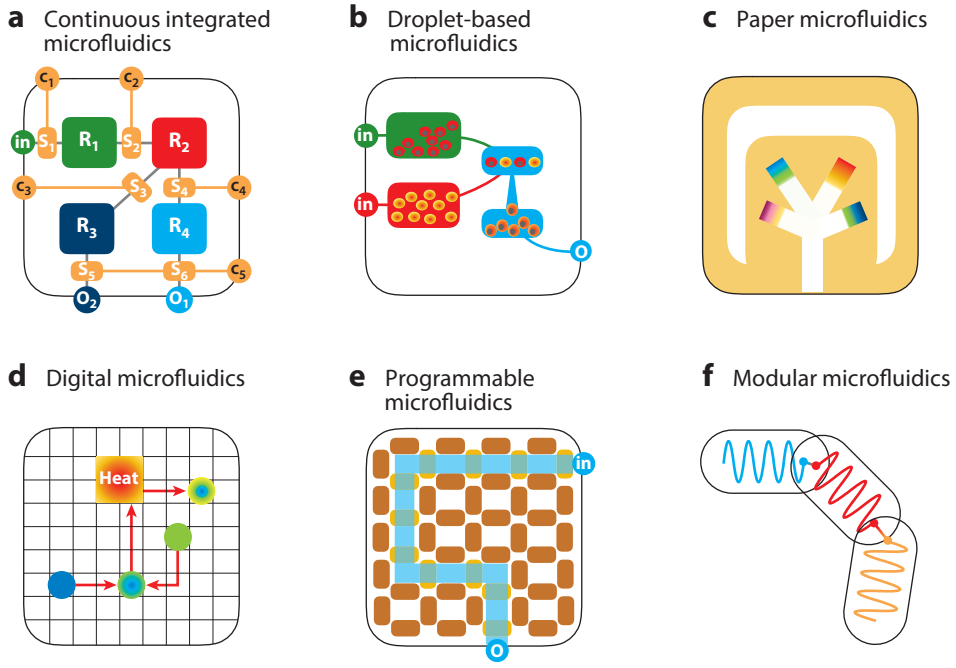

Figure 1

Six paradigms of microfluidics. (*a*) Continuous integrated microfluidics. Fluids flow in closed mechanical channels (*gray*), are controlled using integrated microvalves (*orange*), and are processed within fluid-processing modules ("R"), which are illustrated with rounded rectangles. Control valves are indicated with "S"; pressure inlets for the control valves, with "c"; fluid outlets, with "O"; and fluid input, with "in." (*b*) Droplet-based microfluidics. Drops of fluids are manipulated within immiscible phases. Here, two drop generators produce drops with different compositions; these drops are later fused together and extracted. (*c*) Paper microfluidics. Fluids are passively transported along hydrophobic physical barriers (*brown*) on hydrophilic paper (*white*). Diffused fluids interact with hydrogenated, color-changing reagents. (*d*) Digital microfluidics. Drops are manipulated on a cell grid, with each cell having a controllable level of wetting characteristics. The schematic shows heating and mixing areas. (*e*) Fully programmable valve arrays. These consist of a dense grid of switchable blocks (*orange*) with which fluid (*blue*) can be manipulated in highly configurable and programmable patterns. (*f*) Modular microfluidics. Discrete sensor-embedding three-dimensionally printed fluidic modules can be assembled to form a complete system.

designs (CADs) reflect design rules, physical knowledge, fabrication constraints, material properties, and numerical models. The process, therefore, requires expertise and numerous iterations (15). To ease the process, microfluidic foundries, such as the one at Stanford University, provide template files and guidelines with design rules and embedded constraints (16), but the overall design process is still heavily based on manual effort.

Three significant movements have dramatically impacted the way traditional pattern-based microfluidics are designed.

1. Increasing design intricacy: Most common designs are planar and require convoluted channel routing to interconnect components. To overcome some of the limitations of two-dimensional (2-D) designs, many devices were designed using multilayered architecture, which is more difficult to realize (17). Moreover, microfluidics large-scale integrated (mLSI) devices may have many thousands of integrated micromechanical valves and control components (18). It has been shown that micro/nano fluidic systems follow Moore's law, as valve

densities have increased exponentially with time (19), reaching a value of 1 million valves per cm^2 (20). MLSI designs are rapidly growing in complexity and, therefore, are difficult to define manually.

2. Performance needs: The quest for high-performing microfluidic applications is indicated by their utilization for large volumes and complex fluids (21), as well as for applications in which response time is critical. The latter can be particularly challenging due to three main drawbacks: (*a*) The actuation time of a microfluidic valve is relatively slow, as pressure has to propagate through a control channel; (*b*) set up time has to be fit between consecutive actuation patterns to ensure proper sealing; and (*c*) asynchronous control is often impossible since a series of valves connected to a single pressure line cannot be actuated simultaneously (22). Manually defined designs of microfluidics are suboptimal in terms of size and satisfaction degree of physical, fabrication, and timing constraints. As the performance needs of microfluidic applications become increasingly challenging, the quest for optimization becomes even more apparent.
3. New fabrication paradigms: Most devices are fabricated using soft lithography, which usually takes place in a clean room and requires intensive manual intervention (6). The high costs generally involved with microfluidic design and fabrication hinder its large-scale adoption (23). The traditional microfluidic fabrication paradigm is being revolutionized with the introduction of 3-D printing technologies, with which there is a seamless transition from a CAD file to a functional product (24, 25). An enhanced vision has emerged from this new fabrication paradigm: a smooth transition from specification to a working product. In the framework of this vision, manual intervention is eliminated (26). The vision is further enhanced by an interesting trend, recently described by Walsh and colleagues (27), in which microfluidic fabrication is moving from clean rooms to maker spaces where access to 3-D printers, laser cutters, plotter cutters, and other fabrication tools is affordable.

One reaction to these three movements was the inception of modular microfluidics. For example, Bhargava and colleagues (28) proposed a modular microfluidic system in which discrete, sensor-embedding 3-D-printed fluidic modules can be assembled to form a complete system (**Figure 1*f***); Morgan and colleagues (29) utilized fused filament fabrication to propose a comparable modular microfluidic framework; Yuen and colleagues (30) described a similar system that utilizes leak-free magnetic interconnections to ease the assembly process; and Wang and colleagues (31) used randomly designed microfluidic circuits as elements in a desired application, generating a query database of thousands of numerically evaluated microfluidic designs from which a functional prototype for fabrication can be derived. While modular and random microfluidics offer significant advantages in terms of predictability and design time, they can rarely assemble an optimized system nor satisfy the requirements of demanding performance systems.

This review covers some of the most important directions in computer-aided optimized design of pattern-based microfluidics. The discussion focuses on continuous microfluidics and briefly highlights droplet-based and paper-based microfluidics. Algorithms and design approaches are summarized in **Table 1**.

2. COMPUTER-AIDED DESIGN

Pattern-based microfluidics is predominantly defined via vector graphics, with which geometries are described as a series of parametric equations. This mathematically defined geometrical space opens the door for optimization and automatic synthesis via CAD. CAD has applications in various fields of emerging technologies: from quantum physics, in which the specification of a quantum

Table 1 Algorithms and design approaches for computer-aided microfluidic design

	Microfluidic platform	Name/description	Author(s)	Reference and/or project page
Description languages	Continuous	Microfluidic Instruction Set Architecture (ISA)	Amin et al.	36
		Manifold 2.0	Klassen et al.	37
		MINT	Huang	39
		BioStream	Thies et al.	33
		AquaCore	Amin et al.	40
		BioCoder	Ananthanarayanan & Thies	41
		BioBlocks	Gupta et al.	42
	Droplet	Droplet specification	Grimmer et al.	92
Optimization algorithms	Continuous	Control-centric (number of channels)	Amin et al.	36
		Control-centric (number, response time)	Hu et al.	44
		Control-centric (number of switching activity)	Tseng et al.	47
		Flow-centric (travel length assuming Manhattan distance)	Lin et al.	45
		Flow-centric (travel length with arbitrary angles)	Yang et al.	46
		Flow-centric (travel length via seam carving)	Crites et al.	48
		Real-time execution; parallelization; mutual exclusion	Li et al.	49
		Completion time	Huang et al.	50
		Mixing (via turbulence)	Inguva et al.	51
		Genetic circuits	Huang & Densmore	52
		Flow-control co-optimization (channel-congested regions assuming Manhattan distance)	Wang et al.	54
		Flow-control co-optimization (arbitrary angles, pressure-sharing control channels)	Tseng et al.	55
		Scheduling	Li et al.	56
		Testability	Liu et al.	60
		Fault detection	Liu et al.	61
		Fault tolerance	Araci et al.	62
		Resistive circuits	Tsur & Shamir	78
	Droplet	Travel length	Grimmer et al.	91
		Trapping wells	Grimmer et al.	87
	Paper-based	Sample loss	Nguyen et al.	97
Standards and benchmarks	Continuous	ParchMint	Crites et al.	63
		Boolean algebraic benchmark	Huang & Densmore	52

(*Continued*)

Table 1 (*Continued*)

	Microfluidic platform	Name/description	Author(s)	Reference and/or project page
Design tools	Continuous	Design rules	Stanford University Microfluidics Foundry	16; **https://stanford.ilabsolutions.com/service_center/show_external/22/microfluidics-foundry**
		Micado (AutoCAD plugin)	Amin et al.	36; **http://groups.csail.mit.edu/cag/micado/**
		The Neptune Project	McDaniel et al.	64; **https://github.com/CIDARLAB/Neptune**
		Columba	Tseng et al.	65; **http://tueieda-columba.srv.mwn.de/**
		3DμF	Sanka et al.	66; **https://github.com/CIDARLAB/3DuF**
		Random design	Wang et al.	31; **http://random.groverlab.org/**
	Droplet	Design rules	Glawdel et al.	85
		Droplet generation	Lashkaripour et al.	83
		Experiment design	Grimmer et al.	93
	Paper-based	Design rules	Potter et al.	98
		AutoPAD	DeChiara et al.	99; **https://github.com/MaceLab/AutoPAD**

circuit for a given quantum functionality remains a key topic, to microfluidic networks, in which automated synthesis aims to revolutionize the field with designs that reach pioneering levels of complexity (32).

Particularly, CAD aims to (*a*) enhance layout to realize application provisions and thus improve optimization; (*b*) reduce the manual effort involved in designing intricate devices; and (*c*) enable the realization of the vision in which users specify their requirement set and an optimized device is produced by their desktop 3-D printer. This review argues in favor of a 5-D CAD framework.

1. Description language: Most microfluidic designs are defined using editors into which predefined components may be imported from libraries of microfluidic primitives (e.g., cell traps, mixers, multiplexers, pumps). While optimizing layout design is possible, the true potential of CAD for microfluidics lies within the possibility of laying out an optimal solution given a device or application description. To enable this, hardware description languages were developed. Such languages can use components as pieces of code. Having a consistent and acceptable microfluidic description language is an essential abstraction layer, which will eventually enable microfluidic scaling, as it decouples software development from changes in the technology of the underlying device (33).
2. Design for optimization: CADs can address general microfluidic applications (e.g., FPVA) or, alternatively, focus on a restricted class of functionalities. Usually, designs are optimized for a specific application; for example, if an application requires the sequential mixing of liquid samples, should we design a device with one mixer and one incubation unit to optimize the size of the device, or should more mixers be integrated to optimize the execution time (34)? We might also ask, what is the optimal sequence of operations, or how should we schedule processes in the device to achieve optimal results? Fundamentally, the aim is to factorize the optimization factors with the correctly weighted components (constituting the loss function) to optimize the design.

3. Optimization methods: Optimization methods may be classified into (*a*) iterative methods in which a base solution is improved in a series of approximations until convergence is achieved; (*b*) heuristic-based methods, which provide a fast, approximate good enough solution through a series of educated guesses; and (*c*) exact—that is, analytical—methods, which provide the best possible solution either by exhausting the entire space of possible designs or by solving an analytical description of the problem. The latter is rare in design optimization since the possible-designs space is large and analytical descriptions are scarce. Traditionally, designers have focused primarily on product performance, often neglecting the downstream processes and operations that follow design. Design for X is an integrated approach that extends the definition of design for performance to, for example, design for testability, assembly, simplicity, and serviceability (35). This review also focuses on design for testability and tolerance. This is particularly important for microfluidics as the fabrication process is prone to defects. Therefore, some microfluidic designs consist of specialized pressure inlets, meters, and integrated valves to allow for testability. This design approach optimizes the system such that minimal effort will be needed to evaluate the device following fabrication.
4. Benchmarks: Any microfluidic application can be realized as a design in numerous ways. Moreover, while one design may be ideal for one application, it may perform poorly for another. Therefore, to compare different design optimization methods or to compare design performance against different applications, a benchmark is needed. A microfluidic benchmark is a collection of designs that have been generated for a specific application using different optimization methods. It enables different designs to be compared against known metrics. Benchmarks can be particularly useful when there is a standard that defines the format within which designs are structured, thus providing researchers with a way to conveniently interchange and compare data with each other.
5. Design tools: Using microfluidic description language, optimization algorithms, and benchmarks in CAD are not trivial tasks, primarily since algorithms and benchmarks were designed to be used in a different development environment. A principal design tool is the integrated development environment in which designers can define, optimize, and prepare their device for fabrication.

In the following section, each of these five dimensions is explored in the context of CAD for continuous microfluidic systems.

3. COMPUTER-AIDED DESIGN OF CONTINUOUS MICROFLUIDICS

Continuous (flow-based) microfluidic devices are manufactured using multilayer soft lithography and are composed of two layers: one for flow and the other for control. Valves are formed at the flow–control intersection points, as has been previously described in detail by Melin & Quake (15).

3.1. Description Languages

One of the first attempts to develop a description language for microfluidics was proposed by Amin and colleagues (36) in a framework they termed microfluidic Instruction Set Architecture (ISA). Briefly, the flow layout is described as a series of flows ($F_1 \ldots F_n$) that can be constrained to flow in OR parallel (i.e., fluid streams pass through either F_x or F_y) or in AND parallel (i.e., fluid streams pass simultaneously though both F_x and F_y). A series of such logical statements constitutes the device's layout. Another specification language, termed Manifold 2.0, was more recently described

by Klassen and colleagues (37). Manifold provides a modular approach for microfluidic specification in which primitives such as nodes and ports can be assembled and configured to define reusable microfluidic modules. The authors also developed a compiler, with which the modules can be simulated over MapleSim (38). Another similar, module-based and highly utilized description language is MINT (39). Some efforts have been made to reach higher levels of abstraction and to define the experiment itself with code. The latter will pave the way for a compiler, which would translate an application—or a protocol—to a device. For example, Thies and colleagues (33) developed BioStream, a description language for biological protocols. BioStream specifications can be seamlessly translated to microfluidic ISAs (33). Another development is AquaCore, which is an instruction set for a universal microfluidic layout (40). Since BioStream supports only mixing, storage, detection, and input and output primitives, and AquaCore is limited to a specific fluidic architecture, Ananthanarayanan & Thies (41) developed BioCoder. This is a platform-agnostic description language for complicated procedures, and it may eventually be used for fully automated microfluidic-based execution of arbitrary protocols. As writing code is not intuitive to many experimentalists, Gupta and colleagues (42) proposed a visual programming environment termed BioBlocks, in which experiments are described as a set of interconnected blocks.

3.2. Design for Optimization

A standard scheme for microfluidic CAD and optimization is to (*a*) devise a sequence graph (e.g., mixing, splitting, storing, sensing) that describes a specific application (**Figure 2*a***), (*b*) bind and schedule microfluidic resources for each operation (**Figure 2*b***), (*c*) derive an optimal flow layer by defining the required fluidic modules and their interconnections (**Figure 2*c***), and (*d*) derive an optimal control layer in which the location, addressing method, and routing are computed (43) (**Figure 2*d***).

Optimization can be realized in respect to different design parameters. One of the first attempts to utilize CAD for continuous microfluidics was proposed by Amin and colleagues (36), and it focused on control-layer optimization. Their design methodology was based on an iterative algorithm that minimized the number of control channels. More recently, Hu and colleagues (44) proposed a routing algorithm that relaxed Amin et al.'s assumption of placing the control inlets in the device periphery, thus allowing control inlets to be placed anywhere on the chip. Their

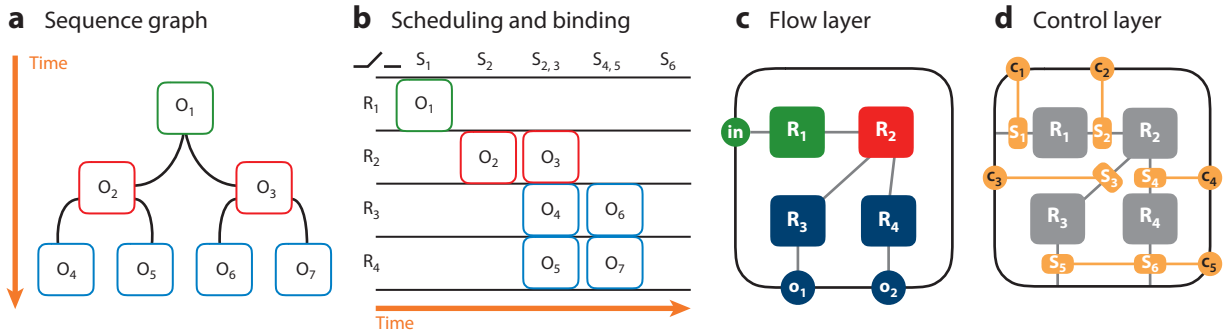

Figure 2

A scheme for microfluidic computer-aided design and optimization. (*a*) A sequence graph featuring three types of processing modules—splitting (*green*), storing (*red*), and sensing (*blue*)—and seven operations ($O_1 \ldots O_7$). (*b*) Binding $O_1 \ldots O_7$ to processing resources ($R_1 \ldots R_3$) and scheduling. For each process, a control sequence is generated (specifying opened valves). (*c*) Flow-layer architecture, featuring processing resources $R_1 \ldots R_3$, inlets, and outlets. (*d*) Control-layer architecture featuring valves ($S_1 \ldots S_6$) and five pressurized control inlets ($c_1 \ldots c_5$).

method optimizes both the number of control pins and the response time (44). Other methods have concentrated on the flow layer. For example, Lin and colleagues (45) proposed an algorithm that minimizes the total length of the flow channels. Recently, Yang and colleagues (46) relaxed key assumptions in previous work of having routes follow Manhattan routing metrics (i.e., straight channels and 90° bends), allowing channel routing at any angle, thus reducing channel length by more than 15%. Tseng and colleagues (47) proposed a valve-centric optimization method in which designs are optimized to minimize valve-switching activities, thus prolonging a device's life span. While most optimization methods rely on a mathematical description of the problem, an interesting and particularly creative approach for optimizing flow layouts was offered by Crites and colleagues (48). They utilized an algorithm from computer graphics termed seam carving, in which an image is resized by an iterative removal of the pixel paths that have the lowest contribution to the image's contrast. The authors used seam carving to significantly reduce the size and total length of the flow channels. Other approaches optimize parallel and real-time execution. For example, Li and colleagues (49) proposed a design methodology that optimized real-time execution, mutual exclusion (i.e., preventing simultaneous access to a shared resource), and parallel execution. Huang and colleagues (50) proposed an algorithm that optimized the study completion time of a prespecified maximal amount of control channels. Some design methodologies focus on specific applications. For example, Inguva and colleagues (51) proposed CAD of microfluidic mixers for protein and RNA studies in which a design is optimized for its ability to introduce and sustain turbulence. Huang and colleagues (52) proposed a framework they termed Fluigi for optimizing the layout of microfluidic genetic circuits. The Fluigi CAD approach is based on the utilization of primitive genetic gates that are organized on a generic microfluidic valve-based fabric. Fluigi was even deployed to a cloud and provided as software as a service for the community (53).

While the above methods optimize either the flow or the control layers, several attempts have been made to perform co-optimization of both layers. This design methodology adjusts component placement based on feedback from both the flow and control layers. For example, Wang and colleagues proposed a placement algorithm in which the location of fluidic components is modified to minimize channel-congested regions (54). A similar approach, termed Columba, was proposed by Tseng and colleagues (55), enhancing Wang's algorithm with angled channel routing and pressure-sharing control channels.

Realizing that microfluidic design often integrates existing modules, Li and colleagues (56) proposed the component-oriented synthesis concept, in which regular microfluidics are described as discrete entities. Particularly, components are classified as (*a*) containers, which are composed of chambers (i.e., channel segments bound with valves and rings, known as circulated flow), (*b*) accessories, which are composed of pumps, heating pads, optical sensing units, sieve valves (i.e., specialized valves that impede the flow of particles), and cell traps. Within this component-oriented approach, operations are defined with a container and accessories, as well as by their duration and dependencies. Operations and their dependencies can constitute the sequence graph, which has to be scheduled on a device. While scheduling resources is a classic algorithmic question in theoretical computer science (57), it has also been extensively discussed for microfluidic design, particularly for digital microfluidics (58). With this approach, design optimization can follow higher levels of specifications to optimize functionality; particularly, a device can be optimized for a pregenerated schedule as well as for real-time decisions. Li and colleagues (56) and others (47) devised an algorithm allowing for both real-time and prescheduled processing (i.e., hybrid scheduling) while optimizing processing for different parameters, such as total execution time and transportation paths in the sequence graph.

Another important aspect is designing for testability and tolerance. Potential device defects include unsealed valves, poor interlayer bonding, misalignment, trapped debris, and channel block

or leak. Some of the defects cannot be visually inspected, and others develop over time (see an extended discussion by Hu and colleagues in Reference 59). As microfluidic applications grow in size and complexity, special flow and control valves need to be introduced to facilitate testing. Liu and colleagues (60) suggested an optimization algorithm that minimizes the number of pressure sources and meters by adding a series of dedicated valves and channels. Designing for testability is particularly important for FPVAs, which decouple an application from the device's architecture, allowing developers to focus on device scalability and testability. By utilizing the concepts of flow paths and cut-sets, Liu and colleagues (61) designed an optimized methodology for fault detection in FPVAs. For general continuous microfluidic designs, Araci and colleagues (62) proposed a fault-tolerant design strategy with which failed valves or channels can be managed. Their approach was to introduce redundancy so as to allow for application execution on a failed device.

3.3. Standards and Benchmarks

Data formats, benchmarks, and metrics are needed to analyze the performance of CAD. Crites and colleagues (63) proposed a standard interchange format they termed ParchMint for continuous microfluidics, which specifies the device netlist (i.e., list of connections) as a JavaScript Object Notation (or JSON) file. This standard describes the device architecture with components, connections, and layers, which together specify the detailed architecture of the device. ParchMint was utilized to create a microfluidic benchmark, which is composed of reverse-engineered published devices (i.e., derived from images), generic grids of cell traps and valves, and other application-derived designs. These designs were mapped to a benchmark space (i.e., specifying the number of components and dimensions), allowing researchers to compare their designs against designs of similar complexity. Some benchmarks are application specific. For example, the Fluigi framework was tested against Boolean algebraic benchmark circuits found in synthetic biology and electrical engineering (52).

3.4. Design Tools

One of the first design tools was proposed by Amin and colleagues (36), integrating their optimization algorithm described above into AutoCAD software (i.e., a design tool) via a plugin termed Micado. One interesting attempt at creating a design suite for continuous microfluidics was initiated at Boston University and termed The Neptune Project (64). In this project, MINT-specified microfluidic designs were automatically translated into design schematics, together with a warning list of design rules that might have been violated during layout. Neptune further allows users to download a CAD file for 3-D printing as well as to control a device's valves through a graphical user interface. Another design tool proposed by Tseng and colleagues (65) is Columba, which is based on co-optimization, as mentioned earlier. The Columba design synthesis tool interprets device specifications into an optimized microfluidic layout and translates that into a series of AutoCAD drawing commands. It enables a seamless translation from specification to device fabrication. One of the most complete and most utilized design synthesis tools is 3DμF, which was recently proposed by Sanka and colleagues (66). 3DμF is an open-source, interactive microfluidic design tool that can be extended to support state-of-the art automation algorithms, fabrication, and control. The framework encodes layout using ParchMint, provides a library of parameterized microfluidic blocks, and supports modular microfluidics.

3.5. Case Study: Computer-Aided Design of Resistive Microfluidic Networks

This section discusses a series of algorithms aimed at using CAD for resistive microfluidic networks (RMNs). RMNs control fluid velocity in individual segments of complex networks to

provide precise transport of fluids (67). They may be of use in various applications, from the generation of chemical gradients for cell migration analysis in chemotaxis studies (68, 69) to the precise control of mixing ratios of fluids for surface modification of nanoparticles (70). Another important application of a flow-rate regulator is to maintain a constant flow rate over pressure variations. A complete solution for CAD of RMNs is composed of four aspects: (*a*) a design for a digitally controlled hydraulic microfluidic resistor; (*b*) utilization of the microfluidic resistor in an optimized RMN layout, realizing a resistance profile that follows high-level description of a desired application; (*c*) synthesis of an optimized device that realizes the RMN layout for 3-D printing; and (*d*) a control framework that aims at adjusting the controllable hydraulic resistance profile to match the desired application. A schematic of this framework is shown in **Figure 3*a***.

3.5.1. Digitally controlled hydraulic microfluidic resistor. In a recent article, I proposed a design for a microfluidic hydraulic resistor (71). This design is based on an analogy to a hydraulic–electric circuit, in which the Hagen–Poiseuille equation, which governs hydraulic behavior, is considered equivalent to Ohm's law, which describes electrical currents in a resistive conductor (72). Under the assumption that flow is laminar, viscous, and incompressible (as is usually the case for flow in microscale networks), voltage drop and electrical resistance can be treated as analogous to, respectively, pressure drop and hydraulic resistance.

Hagen–Poiseuille's law can be used to describe the relation between flow and resistance. Hagen–Poiseuille's law can be expressed as:

$$\mathrm{Q} = \frac{\Delta \mathrm{p}}{\mathrm{R_H}}, \qquad 1.$$

where Q is the volumetric flow rate ($\mathrm{m^3/sec}$), Δp is the pressure difference (Pa), and R is the hydraulic resistance. The hydraulic resistance for rectangular channels—the most common geometry in microfluidic networks–is given by:

$$\mathrm{R_H} = \frac{12\eta \mathrm{L}}{\mathrm{wh}^3\left(1 - \frac{\mathrm{h}}{\mathrm{w}}\left(\frac{192}{\mathrm{n}^5}\sum_{\mathrm{n}=1,3,5}^{\infty}\frac{1}{\mathrm{n}^5}\tan\left[\mathrm{h}\left(\frac{\mathrm{n}\pi\mathrm{w}}{2\mathrm{h}}\right)\right]\right)\right)}, \qquad 2.$$

where η is the fluid viscosity (Pa·sec), and l, w, and h are the channel's length, width, and height (m), respectively.

Our programmable, digitally controlled hydraulic resistor design uses Equations 1 and 2 to feature five linear ranges of resistance, controlled by six to eight control lines, and it can be rapidly embedded within microfluidic designs. The resistor is composed of a series of channels of different lengths that can be combinatorially perfused to gain different fluid resistance values; considering that similarly to electric circuits, parallel connected N fluidic resistors have an equivalent resistance of:

$$\frac{1}{\mathrm{R_{H,T}}} = \frac{1}{\mathrm{R_{H,1}}} + \frac{1}{\mathrm{R_{H,2}}} + \cdots + \frac{1}{\mathrm{R_{H,3}}}.$$

A schematic of the hydraulic resistor is shown in **Figure 3*b***.

3.5.2. Computer-aided design of the layout of an optimized resistive microfluidic network. Following on from this, the programmable resistor was used to provide a methodology for parameter-guided (e.g., flow rate) design of a hydraulic layout (73). This approach concludes the optimal circuit's resistance profile, and it can be adjusted to support different flow constraints

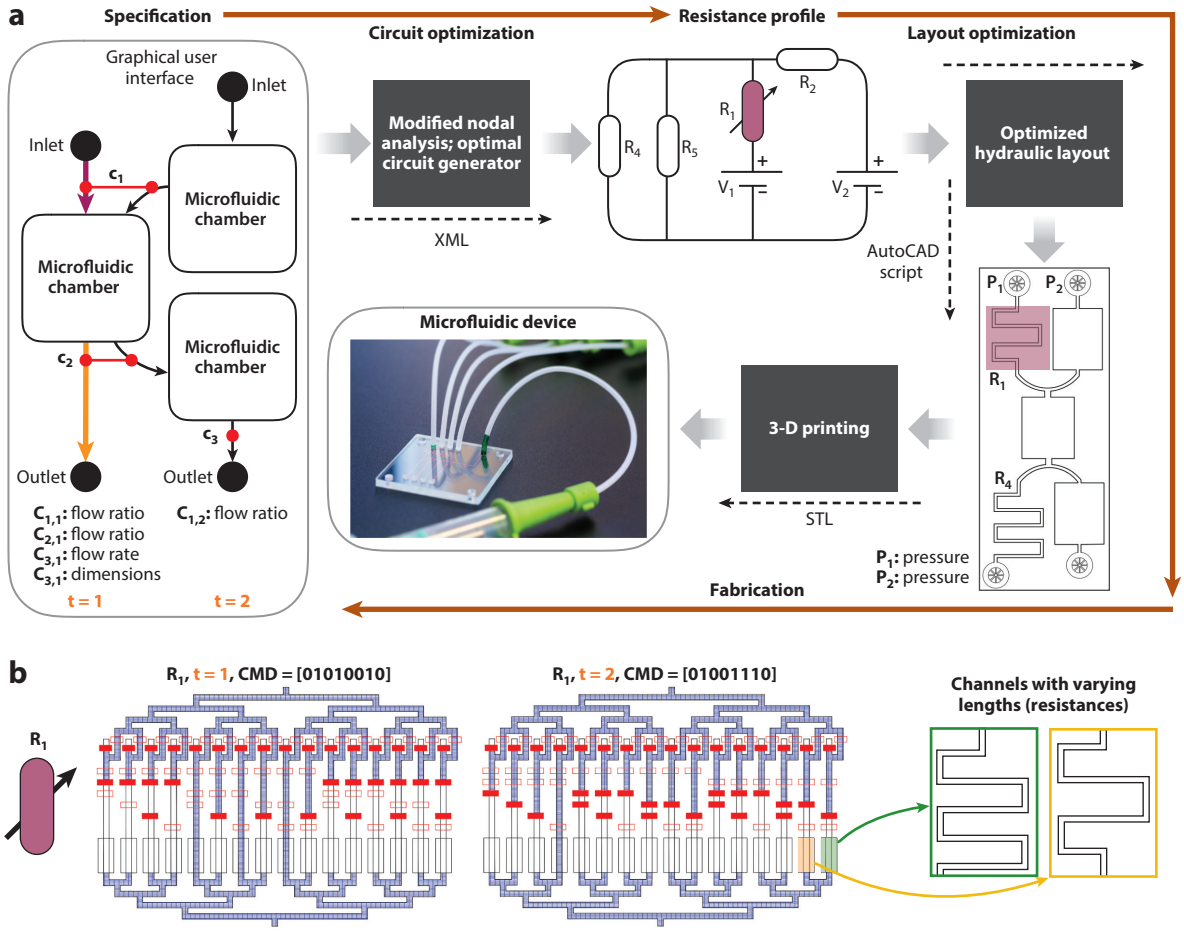

Figure 3

A framework for the computer-aided design of resistive microfluidic networks (RMNs). (*a*) Device specifications and timed (t = 1,2) constraints ($C_{n,t}$) are translated into an optimized resistance profile, which features an adjustable resistor (R_1) (*purple*), to be modified with t and three constant hydraulic resistances ($R_2 \ldots R_4$). The resistance profile is translated into an optimized hydraulic layout, which is suitable for three-dimensional (3-D) printing. (*b*) Design of a digitally controlled hydraulic microfluidic resistor. The schematic shows the hydraulic adjustable resistor controlled by eight control lines (*red*; the closed valve is indicated by *solid red rectangles*; the opened valve is indicated by *red outlined rectangles*). The resistor is composed of a series of channels of different lengths that can be combinatorially perfused to gain different fluid resistance values (examples highlighted in *green* and *orange*). The panel shows the resistors in two configurations (where CMD stands for command), one for each time step.

in varying valve configurations. Initially, the designer schematically defines the desired microfluidic layout, including channels, connections, and valves. Following initialization, the framework tries to solve the network according to the specified parameters and suggests a hydraulic resistance layout, which might also contain hydraulic resistors. To automatically suggest a hydraulic–electric layout that satisfies the designer's constraints, we utilized the modified nodal analysis algorithm (74). In this example, we altered the modified nodal analysis methodology so that currents would be given as parameters, and the hydraulic resistance profile as a solution, thus further extending it to support (*a*) impossible user-defined specifications, (*b*) overdetermined systems (i.e., for which no solution exists for the specified parameters), and (*c*) underdetermined systems (i.e., for which

more than one solution exists for the specified parameters). A full description of the algorithm is given in Reference 73.

3.5.3. Control framework. Conventionally, mLSIs are digitally controlled with a dedicated microprocessor (75, 76). Intricate RMNs, which might include multiple programmable resistors, use the same control methodology. Therefore, we proposed a framework that supports local as well as remote control of flow and data acquisition from multiple resistors. Our system is composed of a pneumatic layout for fluid perfusion and valve actuation, an embedded controller, and a software package that implements and integrates multiple control sources. We use this control system to script a regulation scheme for our hydraulic microscale resistor to provide real-time modulation of flow within a microfluidic network (77).

3.5.4. Synthesis of a resistive microfluidic network device for 3-D printing. Recently, in a work described in the journal *Computer-Aided Design*, we proposed an algorithmic approach for designing RMNs that uses a hydraulic resistance profile to synthesize a microfluidic design for 3-D printing (78). Our algorithm uses fabrication-related constraint propagation and an optimization protocol to suggest a physical design with a minimal footprint for the proposed input electrical model. The algorithm is composed of the following stages: (*a*) construction of snakes' (i.e., flow segment) geometries, one for each resistor in the electrical model, in correspondence with physical and fabrication constraints; (*b*) discretization of the hydraulic layout to a rectangular grid, in correspondence with the dimensions of the channels as they were defined in step *a*; (*c*) random assignment of resistors to the grid; (*d*) optimization of layout through rearrangement of channels' locations; (*e*) channel clustering into nonintersecting groups, in which each group defines one connection layer; (*f*) generation of a layered layout, in which the bottom layer defines the circuit hydraulic channels and the upper layers implement the connection scheme; and (*g*) generation of the design in vector graphics.

Our layout optimization approach aims at reducing the number of intersections of the connections by changing the locations of the flow segments (i.e., the snakes) in the flow layer and then clustering the nonintersecting connecting channels into a minimal number of groups. The snakes shift locations following an optimization protocol aimed at minimizing two cost functions. In this work, we proposed a two-step cost estimation. The parameter for the first cost estimation, *fa*, is the total number of intersections of all connecting channels. This is to rationalize the heuristic that a minimal number of layers is gained via a minimal number of intersections. We further optimize the designs for the best performance according to *fa* by using a second cost estimation, *fb*, which is defined as the total length of the connecting channels. Minimizing *fb* promotes designs in which closely connected channels are packed together. We chose four different protocols to optimize both cost functions. (*a*) Hill climbing occurs when a design is continuously refactored in the direction of increasing value (in terms of the cost function)—that is, uphill. It terminates when it reaches a peak where no neighbor has a higher value. Hill climbing does not look beyond the immediate neighbors of the current state and can, therefore, get stuck in local maxima, ridges, and plateaus. (*b*) Iterative local search is a variant of hill climbing, in which a series of hill-climbing searches are conducted from randomly generated initial states. (*c*) Simulated annealing behaves similarly to hill climbing, with the exception of accepting downhill moves with a probability defined as a function of time (thus, allowing completeness). (*d*) In beam search a search graph is explored by expanding the most-suitable candidate in a limited set (beam diameter). Detailed descriptions of the algorithms can be found in Reference 79. In each step of the optimization cycle, a snake's location is changed, and the total cost is recalculated. These two approaches—that is, CAD of an optimized RMN layout and synthesis of an RMN device for 3-D printing—might

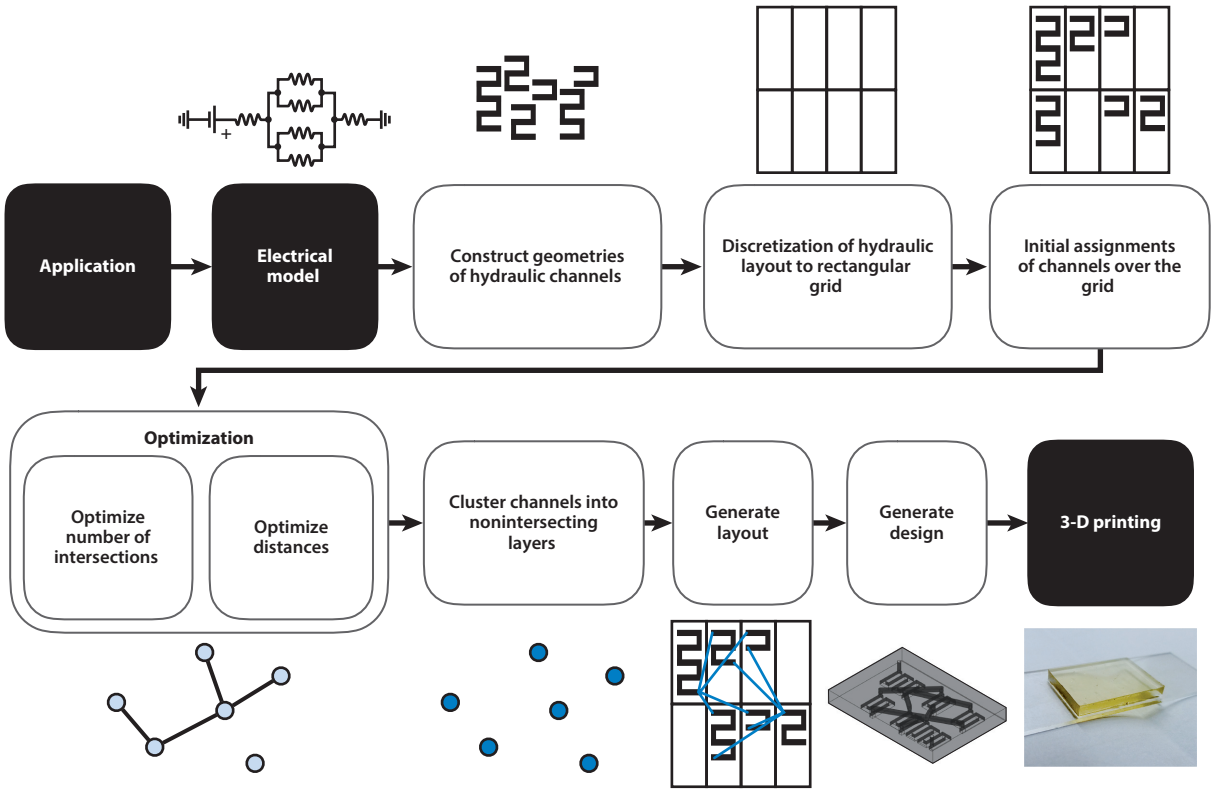

Figure 4

An algorithmic approach for designing resistive microfluidic networks. Following the derivation of an electrical description of the microfluidic application, snakes' (i.e., flow segment) geometries are generated and placed on a discretized hydraulic layout. Snakes shift location according to an optimization search-based algorithm until a final layout is derived. Finally, the layout is generated and exported for fabrication.

work together to allow for a streamlined, optimized design process for RMNs. A schematic of this framework is shown in **Figure 4**.

4. COMPUTER-AIDED DESIGN OF DROPLET-BASED MICROFLUIDICS

In droplet-based microfluidics, subnanoliter droplets are produced within microfluidic components, providing miniature encapsulated environments, within which biological, chemical, and physical experiments can be executed (80). Droplets are guided within a microfluidic network though either active (i.e., via valves or externally applied forces) control or passive (i.e., via hydrodynamic principles) control. For the latter, channel geometry and the consequent hydrodynamic forces are critical design parameters (81).

A key component of droplet-based microfluidics is the droplet generator (82). The two main parameters of a droplet generator are the droplet size and the generation rate, both of which depend on the generator's geometry and flow rates. Recently, Lashkaripour and colleagues (83) proposed a design automation tool for droplet generators using a predictive model: Given the performance required of the generator, the model can predict the relevant geometric and physical parameters. They used regression models, such as M5P trees, and radial basis function

interpolation on thousands of experimental observations. However, this approach is not guided by a physical model of droplet dynamics. The design challenge for droplet-based microfluidics is complex since simulating or modeling droplet behavior is not a trivial task, and it is not readily addressable by current modeling environments (84). Glawdel and colleagues (85) proposed a set of rules to guide designers into a limited relevant design space. This design space, however, has to be experimentally explored. An essential starting point for CAD of droplet-based microfluidics is a relevant framework for its evaluation. Such a framework was proposed by Gleichmann and colleagues (86) who utilized the hydraulic–electric circuit analogy (mentioned above) to model the movement of droplets through a microfluidic network. More recently, Grimmer and colleagues (87) investigated how a similar modeling environment (88) could aid in optimizing a design for droplet-trapping wells, in which droplets from separate streams can get trapped, merge, and mix. The authors utilized a droplet's size, fabrication resolution limits, and the properties of the phases being studied to validate an initial design and to approach three optimization questions: (*a*) What is the minimal bypass channel length (an essential component for a functional trapping device)? (*b*) What is the maximum allowable pressure for N sets of trapping wells? (*c*) How many trapping wells can be cascaded and loaded by droplets in a given time? These questions were iteratively explored in simulations for design optimization.

One of the major advantages of droplet-based microfluidics is its ability to generate an immense amount of droplets quickly (e.g., some generators exceed 10^5 droplets per second) (89), thus enabling high-throughput discovery frameworks (90). Therefore, routing drops through a passive control in a microfluidic setting is highly desirable. However, routing droplets in a network is difficult due to the intricacy of droplet dynamics, which are highly dependent on the droplets themselves as they increase the resistance of a channel owing to their viscosity, size, and geometry. This is particularly hard when the desired application is composed of multiple modules. Grimmer and colleagues (91) proposed a satisfiability-solver-based design algorithm that minimized droplet travel length, the number of channels, the number of modules, and the number of times a channel is passed by a droplet (i.e., to minimize contamination). The resultant architecture can be automatically dimensionalized into a full specification of the device (92). Finally, a droplet sequence ensuring that each droplet is routed to its intended location must be set and evaluated. Such automation of experimental design has also been recently discussed (93).

5. COMPUTER-AIDED DESIGN OF PAPER MICROFLUIDICS

Paper microfluidic devices are small, disposable, made from low-cost material, often have an embedded dehydrated reagent, and can integrate a readout via a color change. Therefore, they hold promise for fulfilling the World Health Organization's ASSURED criteria of being affordable, sensitive, specific, user-friendly, rapid, equipment-free, and delivered to those in need (94). However, similar to continuous and droplet-based microfluidics, paper-based devices are usually manually defined. In paper microfluidics, fluid is driven by capillary forces. Modeling 2-D capillary transportation of fluids is essential for engineering the design and optimization of paper microfluidics. Transport in 2-D paper networks was studied by Fu and colleagues (95) and later by Elizalde and colleagues (96), both providing a rational basis for experiments, analytical expressions, and computational simulation.

One aspect that is unique to the design of paper-based microfluidics is that fluid samples are lost during transportation. The amount of material lost during transport along a 30 mm channel can reach up to 50%. Addressing this issue, Nguyen and colleagues (97) reported on a set of design

rules to aid the optimization of paper-based microfluidics via the introduction of a waste zone, which defines a bigger detection zone, and by using elution steps.

Specialized frameworks were recently proposed for the design of paper microfluidics. Potter and colleagues (98) proposed a framework that uses a library of parameterized paper microfluidic components, which can be rapidly assembled into new devices. Another design framework, termed AutoPAD, was proposed by DeChiara and colleagues (99). In AutoPAD, an open software platform, designs are specified as a set of hierarchies between conventional connected components and exported cutting pattern outlines, which can be vectorized to work with a cutting plotter or laser cutter. While both of these frameworks proved useful, they do not currently support placement and routing algorithms, nor do they offer end-to-end design automation.

Studies have highlighted the promise of using multilayer paper microfluidics—that is, realizing small 3-D designs in which multiple samples can be transported in complex patterns (100). It was later demonstrated that 3-D paper microfluidics can be defined via the principles of origami over a single piece of paper that is folded to create a multilayer structure (101). AutoPAD supports origami-based designs, allowing layer arrangement in a grid, which can then be printed and folded. Since CAD of origami-based shapes is well established (102), CAD origami for paper microfluidics might pave the way for new optimization methods.

6. PERSPECTIVES

Five perspectives on the CAD of microfluidic circuits are outlined in this section and in **Figure 5**.

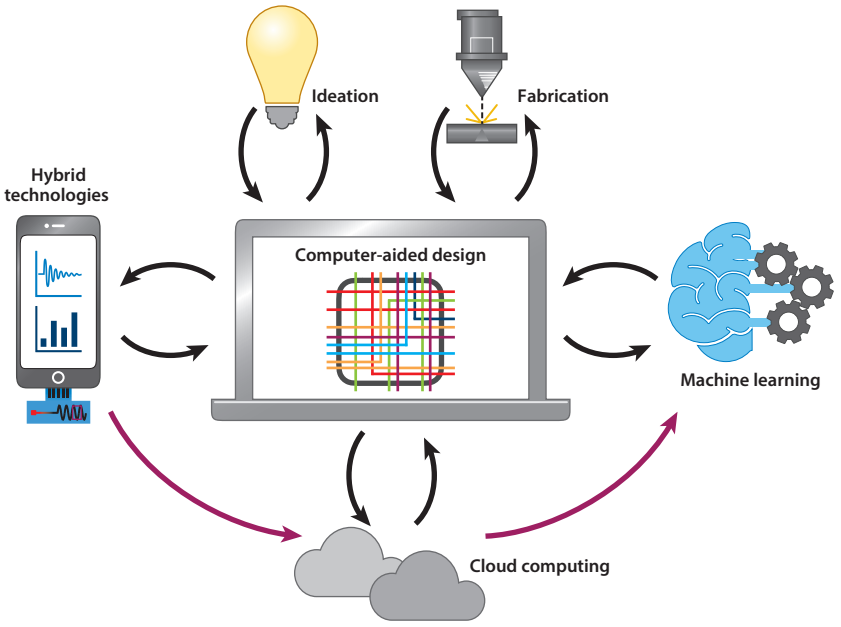

Figure 5

Schematic of the five proposed perspectives on utilizing computer-aided design in microfluidics, including new ideation processes, new fabrication tools, the optimization of hybrids, and the utilization of cloud resources, and machine learning.

6.1. From Integrated Circuits to Microfluidics

George Whitesides, one of the founding fathers of microfluidics, recently stated that microfluidics has passed its first methodological level to become large-scale, and it has finally reached the expensive engineering, production, and market-development wall (103). For the purpose of this discussion, a clear parallel is drawn between microelectronics and microfluidics. CAD is powering the ever-increasing scale of integrated circuits (104) and printed circuit boards (PCBs) (105) in the microelectronics industry. CAD, coupled with advanced fabrication, has liberated PCB design from adhesive tape, pads, and hours of manual cutting, placing, ripping, and routing (106). Similarly, CAD has enabled the design of integrated circuits to encompass countless components and to support 3-D fabrication. There is likely to be a similar impact on microfluidics, helping it to break through the aforementioned engineering wall. CAD will leverage advancements in microfluidics fabrication and integration to provide circuits with unprecedented levels of complexity and functionality, thus realizing microfluidics' immense potential (107).

6.2. Hybrid Optimization and 3-D Fabrication

CAD provides a clear path to microfluidics optimization. Recent advances (highlighted above) have concentrated on high-level optimization, ranging from application to device realization. Some approaches highlight hybrid optimization, as in optimizing both control and flow layers simultaneously. Hybrid optimization is anticipated to go a step further. For example, some designs integrate microfluidics with PCBs (i.e., lab-on-PCB approaches), offering a new level of integration of sensors and electronics (108). Others suggest an integration with smartphones, which can offer accessible control and smart analytics (109). Hybrid optimization is further enhanced by new fabrication paradigms. For example, microfluidic channels can exhibit nonplanar geometries through the design of 3-D scaffolds with arbitrary shapes (110), as well through fabrication directly on microelectronics (111). Other methodologies offer fabrication for tubular elastic microfluidics, which would allow for integration within fabrics and sensors (112). Advances in hybrid optimization may bring microfluidics to a new level of functionality.

6.3. Computer-Aided Design for Design Ideation

Ideation is not commonly discussed in the context of microfluidic design. Lee and colleagues (113) recently explored design strategies for microfluidics. They discussed strategies involving changes in flexibility, geometry, and biological mimicry. CAD might enhance these design strategies by making it easy to introduce changes and providing ways to follow existing design concepts. CAD is traditionally viewed as a closed, mechanical framework, unsuitable for conceptual design (114). However, recent studies have shown that CAD has the potential to support serendipity and provide an environment for creativity and playfulness (115). Therefore it is likely that CAD will not only have an impact on but also enrich microfluidic ideation, as it has done for other engineering disciplines (116). Furthermore, CAD supports a collaborative design process, and this can play an essential role in microfluidic design due to the inherently multidisciplinary nature of microfluidics. CAD support for collaboration was found to be particularly strong in fields in which it is especially hard to manually sketch designs, as in the case of microfluidics. Utilizing CAD at the stage of microfluidic conceptual design will likely enhance the process and advance it toward unconventional and creative routes.

6.4. Machine Learning

Machine learning has been utilized for design in many settings. For example, genetic algorithms have often been utilized for design challenges (117), such as the derivation of new designs for

digital circuits (118). Machine learning was also utilized to automate the design of electronic circuits (119), as well as to optimize mechanical designs (120, 121). The application of machine learning to microfluidics was first demonstrated by Lore and colleagues (122), who showed how neural networks can be exploited to efficiently design pillar sequences for user-defined flow deformations. Furthermore, in the case study described above, a local search algorithm was used to optimize the placement of hydraulic resistors in RMNs (71). Other, more general-purpose seeds were planted recently in work by Lashkaripour and colleagues (123), which demonstrated the possibility of developing a framework for automating modular microfluidic design using machine learning. Therefore, it is likely that the utilization of machine learning for microfluidic design will become more pronounced and apparent.

6.5. Cloud Computing

Cloud-based design and manufacturing is a new paradigm in design innovation, and it is predicted to significantly drive forward digital manufacturing (124, 125). An important example of cloud-based CAD is the highly utilized Autodesk software program Fusion 360, which allows designers to take advantage of virtually unlimited computing power to design highly detailed structures (126, 127). As microfluidic fabrication moves out into maker spaces, tools such as Fusion 360—which integrates cloud CAD, cloud resources, and planning for manufacturing—will increasingly be utilized for microfluidics. The utilization of cloud-powered design for microfluidic design is already taking place, as in the case of the Fluigi cloud described above (53). Continuously growing use of the cloud to support microfluidics design is anticipated.

DISCLOSURE STATEMENT

The author is not aware of any affiliations, memberships, funding or financial holdings that may be perceived as affecting the objectivity of this review.

ACKNOWLEDGMENTS

The author would like to thank Tamara Pearlman Tsur for her insightful comments. This work was supported by the Open University of Israel research grant.

LITERATURE CITED

1. Ranzani T, Russo S, Bartlett NW, Wehner M, Wood RJ. 2018. Increasing the dimensionality of soft microstructures through injection-induced self-folding. *Adv. Mater.* 30(38):1802739
2. Smits J, Damron JT, Kehayias P, McDowell AF, Mosavian N, et al. 2019. Two-dimensional nuclear magnetic resonance spectroscopy with a microfluidic diamond quantum sensor. *Sci. Adv.* 5(7):eaaw7895
3. Streets AM, Zhang X, Cao C, Pang Y, Wu X, et al. 2014. Microfluidic single-cell whole-transcriptome sequencing. *PNAS* 111(19):7048–53
4. Jung W, Han J, Choi J-W, Ahn CH. 2015. Point-of-care testing (POCT) diagnostic systems using microfluidic lab-on-a-chip technologies. *Microelectron. Eng.* 132:46–57
5. Yeh E-C, Fu C-C, Hu L, Thakur R, Feng J, Lee LP. 2017. Self-powered integrated microfluidic point-of-care low-cost enabling (SIMPLE) chip. *Sci. Adv.* 3(3):e1501645
6. Duffy DC, McDonald JC, Schueller OJ, Whitesides GM. 1998. Rapid prototyping of microfluidic systems in poly(dimethylsiloxane). *Anal. Chem.* 70(23):4974–84
7. Unger MA, Chou H-P, Thorsen T, Scherer A, Quake SR. 2000. Monolithic microfabricated valves and pumps by multilayer soft lithography. *Science* 288(5463):113–16

8. Schneider T, Kreutz J, Chiu DT. 2013. The potential impact of droplet microfluidics in biology. *Anal. Chem.* 85(7):3476–82
9. Martinez AW, Phillips ST, Whitesides GM. 2008. Three-dimensional microfluidic devices fabricated in layered paper and tape. *PNAS* 105(50):19606–11
10. Choi K, Ng AH, Fobel R, Wheeler AR. 2012. Digital microfluidics. *Annu. Rev. Anal. Chem.* 5:413–40
11. Fobel R, Kirby AE, Ng AH, Farnood RR, Wheeler AR. 2014. Paper microfluidics goes digital. *Adv. Mater.* 26(18):2838–43
12. Fidalgo LM, Maerkl SJ. 2011. A software-programmable microfluidic device for automated biology. *Lab Chip* 11(9):1612–19
13. Silva R, Bhatia S, Densmore D. 2016. A reconfigurable continuous-flow fluidic routing fabric using a modular, scalable primitive. *Lab Chip* 16(14):2730–41
14. Ibrahim M, Chakrabarty K, Schlichtmann U. 2017. *CoSyn: efficient single-cell analysis using a hybrid microfluidic platform*. Paper presented at Design, Automation & Test in Europe (DATE), Lausanne, March 27–31
15. Melin J, Quake SR. 2007. Microfluidic large-scale integration: the evolution of design rules for biological automation. *Annu. Rev. Biophys.* 36:213–31
16. Foundry SM. 2019. Designing Your Own Device: Basic Design Rules. [Online]. Available: **https://stanford.ilabsolutions.com/service_center/show_external/22/microfluidics-foundry#Foundry_Design_BasicRules**
17. Glick CC, Srimongkol MT, Schwartz AJ, Zhuang WS, Lin JC, et al. 2016. Rapid assembly of multilayer microfluidic structures via 3D-printed transfer molding and bonding. *Microsyst. Nanoeng.* 2:16063
18. Thorsen T, Maerkl SJ, Quake SR. 2002. Microfluidic large-scale integration. *Science* 298(5593):580–84
19. Hong JW, Quake SR. 2003. Integrated nanoliter systems. *Nat. Biotechnol.* 21(10):1179–83
20. Araci IE, Quake SR. 2012. Microfluidic very large scale integration (mVLSI) with integrated micromechanical valves. *Lab Chip* 12(16):2803–6
21. Toner M. 2018. "Extreme" microfluidics: large-volumes and complex fluids. arXiv:1802.05600v1 [physics.flu-dyn]
22. Hu K, Chakrabarty K, Ho T-Y. 2017. Control-layer optimization. In *Computer-Aided Design of Microfluidic Very Large Scale Integration (mVLSI) Biochips: Design Automation, Testing, and Design-for-Testability*, pp. 25–52. Cham, Switz.: Springer
23. Whitesides GM. 2013. Cool, or simple and cheap? Why not both? *Lab Chip* 13(1):11–13
24. Naderi A, Bhattacharjee N, Folch A. 2019. Digital manufacturing for microfluidics. *Annu. Rev. Biomed. Eng.* 21:325–64
25. Bhattacharjee N, Urrios A, Kang S, Folch A. 2016. The upcoming 3D-printing revolution in microfluidics. *Lab Chip* 16(10):1720–42
26. Waldbaur A, Carneiro B, Hettich P, Wilhelm E, Rapp BE. 2013. Computer-aided microfluidics (CAMF): from digital 3D-CAD models to physical structures within a day. *Microfluid. Nanofluidics* 15(5):625–35
27. Walsh DI III, Kong DS, Murthy SK, Carr PA. 2017. Enabling microfluidics: from clean rooms to makerspaces. *Trends Biotechnol.* 35(5):383–92
28. Bhargava KC, Thompson B, Malmstadt N. 2014. Discrete elements for 3D microfluidics. *PNAS* 111(42):15013–18
29. Morgan A, San Jose L, Jamieson W, Wymant J, Song B, et al. 2016. Simple and versatile 3D printed microfluidics using fused filament fabrication. *PLOS ONE* 11(4):e0152023
30. Yuen PK. 2016. A reconfigurable stick-n-play modular microfluidic system using magnetic interconnects. *Lab Chip* 16(19):3700–7
31. Wang J, Brisk P, Grover WH. 2016. Random design of microfluidics. *Lab Chip* 16(21):4212–19
32. Wille R, Li B, Schlichtmann U, Drechsler R. 2016. *From biochips to quantum circuits: computer-aided design for emerging technologies*. Paper presented at 35th International Conference on Computer-Aided Design, Austin, TX, November 7–10
33. Thies W, Urbanski JP, Thorsen T, Amarasinghe S. 2008. Abstraction layers for scalable microfluidic biocomputing. *Nat. Comput.* 7(2):255–75
34. Tseng T-M, Li B, Schlichtmann U, Ho T-Y. 2015. Storage and caching: synthesis of flow-based microfluidic biochips. *IEEE Des. Test* 32(6):69–75

35. Gatenby DA, Foo G. 1990. Design for X (DFX): key to competitive, profitable products. *AT&T Tech. J.* 69(3):2–13
36. Amin N, Thies W, Amarasinghe S. 2009. Computer-aided design for microfluidic chips based on multilayer soft lithography. In *IEEE International Conference on Computer Design*, pp. 2–9. New York: IEEE (Inst. Electr. Electron. Eng.)
37. Klassen N, Lyons M, Prysiazny M, Roth P, Socha P, et al. 2017. *Manifold 2.0: a hardware description language for microfluidic devices*. Paper presented at IEEE 30th Canadian Conference on Electrical and Computer Engineering, Windsor, Ontario, April 30–May 3
38. Hřebíček J, Řezáč M. 2008. *Modelling with Maple and MapleSim*. Paper presented at 22nd European Conference on Modelling and Simulation, Nicosia, Cyprus, June 3–6
39. Huang H. 2016. *Fluigi: an end-to-end software workflow for microfluidic design*. Dissertation, Boston Univ.
40. Amin AM, Thottethodi M, Vijaykumar TN, Wereley S, Jacobson SC. 2007. AquaCore: a programmable architecture for microfluidics. *ACM SIGARCH Comput. Arch. News* 35(2):254–65
41. Ananthanarayanan V, Thies W. 2010. BioCoder: a programming language for standardizing and automating biology protocols. *J. Biol. Eng.* 4(1):13. **https://doi.org/10.1186/1754-1611-4-13**
42. Gupta V, Irimia J, Pau I, Rodriguez-Paton A. 2017. BioBlocks: programming protocols in biology made easier. *ACS Synth. Biol.* 6(7):1230–32
43. Yao H, Wang Q, Ru Y, Cai Y, Ho T-Y. 2015. Integrated flow-control codesign methodology for flow-based microfluidic biochips. *IEEE Des. Test* 32(6):60–68
44. Hu K, Dinh TA, Ho T-Y, Chakrabarty K. 2016. Control-layer routing and control-pin minimization for flow-based microfluidic biochips. *IEEE Trans. Comput. Aided Des. Integr. Circuits Syst.* 36(1):55–68
45. Lin C-X, Liu C-H, Chen I-C, Lee DT, Ho T-Y. 2014. *An efficient bi-criteria flow channel routing algorithm for flow-based microfluidic biochips*. Paper presented at 51st ACM/EDAC/IEEE Design Automation Conference, San Francisco, CA, 1–5 June
46. Yang K, Yao H, Ho T-Y, Xin K, Cai Y. 2018. AARF: any-angle routing for flow-based microfluidic biochips. *IEEE Trans. Comput. Aided Des. Integr. Circuits Syst.* 37(12):3042–55
47. Tseng K-H, You S-C, Minhass WH, Ho T-Y, Pop P. 2013. *A network-flow based valve-switching aware binding algorithm for flow-based microfluidic biochips*. Paper presented at 18th Asia and South Pacific Design Automation Conference (ASP-DAC), Yokohama, Japan, January 22–25
48. Crites B, Kong K, Brisk P. 2017. *Reducing microfluidic very large scale integration (mVLSI) chip area by seam carving*. Paper presented at Great Lakes ACM Symposium on VLSI, Banff, Alberta, May 10–12
49. Li M, Tseng T-M, Li B, Ho T-Y, Schlichtmann U. 2016. *Sieve-valve-aware synthesis of flow-based microfluidic biochips considering specific biological execution limitations*. Paper presented at Design, Automation & Test in Europe Conference & Exhibition (DATE), Dresden, Germany, March 14–18
50. Huang X, Ho T-Y, Guo W, Li B, Schlichtmann U. 2019. *MiniControl: synthesis of continuous-flow microfluidics with strictly constrained control ports*. Paper presented at 56th *ACM/IEEE Design Automation Conference (DAC)*, Las Vegas, June 2–6
51. Inguva V, Kathuria SV, Bilsel O, Perot BJ. 2018. Computer design of microfluidic mixers for protein/RNA folding studies. *PLOS ONE* 13(6):e0198534
52. Huang H, Densmore D. 2014. Fluigi: microfluidic device synthesis for synthetic biology. *ACM J. Emerg. Technol. Comput. Syst.* 11(3):26
53. Subacius K, Kapadia P, McCormack S, Asthana A, Sanka R, Densmore D. 2017. *Fluigi Cloud—a cloud CAD platform for microfluidics*. Poster presented at 9th International Workshop on Bio-Design Automation (IWBDA), Pittsburgh, PA, 2017
54. Wang Q, Zou H, Yao H, Ho T-Y, Wille R, Cai Y. 2017. Physical co-design of flow and control layers for flow-based microfluidic biochips. *IEEE Trans. Comput. Aided Des. Integr. Circuits Syst.* 37(6):1157–70
55. Tseng T-M, Li M, Li B, Ho T-Y, Schlichtmann U. 2016. *Columba: co-layout synthesis for continuous-flow microfluidic biochips*. Paper presented at 35th International Conference on Computer-Aided Design, Austin, TX, November 7–10
56. Li M, Tseng T-M, Li B, Ho T-Y, Schlichtmann U. 2017. *Component-oriented high-level synthesis for continuous-flow microfluidics considering hybrid-scheduling*. Paper presented at 54th ACM/EDAC/IEEE Design Automation Conference, Austin, TX, June 18–22

57. Brucker P, Drexl A, Möhring R, Neumann K, Pesch E. 1999. Resource-constrained project scheduling: notation, classification, models, and methods. *Eur. J. Oper. Res.* 112(1):3–41
58. Su F, Chakrabarty K. 2004. *Architectural-level synthesis of digital microfluidics-based biochips*. Paper presented at IEEE/ACM International Conference on Computer-Aided Design, San Jose, CA, November 7–11
59. Hu K, Yu F, Ho T-Y, Chakrabarty K. 2014. Testing of flow-based microfluidic biochips: fault modeling, test generation, and experimental demonstration. *IEEE Trans. Comput. Aided Des. Integr. Circuits Syst.* 33(10):1463–75
60. Liu C, Li B, Ho T-Y, Chakrabarty K, Schlichtmann U. 2018. *Design-for-testability for continuous-flow microfluidic biochips*. Paper presented at 55th ACM/EDAC/IEEE Design Automation Conference, June 24–28
61. Liu C, Li B, Bhattacharya BB, Chakrabarty K, Ho T-Y, Schlichtmann U. 2017. *Testing microfluidic fully programmable valve arrays (FPVAs)*. Paper presented at Design, Automation & Test in Europe (DATE), Lausanne, March 27–31
62. Araci IE, Pop P, Chakrabarty K. 2015. *Microfluidic very large-scale integration for biochips: technology, testing and fault-tolerant design*. Paper presented at 20th IEEE European Test Symposium (ETS), Cluj-Napoca, Romania, May 25–29
63. Crites B, Sanka R, Lippai J, McDaniel J, Brisk P, Densmore D. 2018. *ParchMint: a microfluidics benchmark suite*. Paper presented at IEEE International Symposium on Workload Characterization (IISWC), Raleigh, NC, September 30–October 2
64. McDaniel J, Grover WH, Brisk P. 2017. *The case for semi-automated design of microfluidic very large scale integration (mVLSI) chips*. Paper presented at Design, Automation & Test in Europe (DATE), Lausanne, March 27–31
65. Tseng T-M, Li M, Freitas DN, McAuley T, Li B, et al. 2017. Columba 2.0: a co-layout synthesis tool for continuous-flow microfluidic biochips. *IEEE Trans. Comput. Aided Des. Integr. Circuits Syst.* 37(8):1588–601
66. Sanka R, Lippai J, Samarasekera D, Nemsick S, Densmore D. 2019. 3DμF—interactive design environment for continuous flow microfluidic devices. *Sci. Rep.* 9:9166
67. Choi S, Lee MG, Park J-K. 2010. Microfluidic parallel circuit for measurement of hydraulic resistance. *Biomicrofluidics* 4(3):034110
68. Sun K, Wang Z, Jiang X. 2008. Modular microfluidics for gradient generation. *Lab Chip* 8(9):1536–43
69. Tsur EE, Zimerman M, Maor I, Elrich A, Nahmias Y. 2017. Microfluidic concentric gradient generator design for high-throughput cell-based studies. *Front. Bioeng. Biotechnol.* 5:21
70. Jahn A, Reiner JE, Vreeland WN, DeVoe DL, Locascio LE, Gaitan M. 2008. Preparation of nanoparticles by continuous-flow microfluidics. *J. Nanoparticle Res.* 10(6):925–34
71. Tsur EE. 2016. Computer-aided design of a microscale digitally controlled hydraulic resistor. *IEEE Trans. Comput. Aided Des. Integr. Circuits Syst.* 36(3):508–12
72. Oh KW, Lee K, Ahn B, Furlani EP. 2012. Design of pressure-driven microfluidic networks using electric circuit analogy. *Lab Chip* 12(3):515–45
73. Feinerman O, Sofer M, Tsur EE. 2018. *Computer-aided design of valves-integrated microfluidic layouts using parameter-guided electrical models*. Paper presented at 5th Joint US–European Fluids Engineering Division Summer Meeting, Montreal, Quebec, July 15–20
74. Ho C-W, Ruehli A, Brennan P. 1975. The modified nodal approach to network analysis. *IEEE Trans. Circuits Syst.* 22(6):504–9
75. Ezra E, Maor I, Bavli D, Shalom I, Levy G, et al. 2015. Microprocessor-based integration of microfluidic control for the implementation of automated sensor monitoring and multithreaded optimization algorithms. *Biomed. Microdevices* 17(4):82
76. Ezra E, Bavli D, Nahmias Y. 2016. Integrated control of microfluidics—application in fluid routing, sensor synchronization, and real-time feedback control. In *Advances in Microfluidics: New Applications in Biology, Energy, and Materials Sciences*, ed. XY Yu, p. 165. London: IntechOpen
77. Arfi N, Tsur EE. 2017. Programmable multi-source embedded control of large-scale integrated microfluidic circuits with an application for real time flow rate modulation. Paper presented at 3rd International Conference on Control, Automation and Robotics (ICCAR), Nagoya, Japan, April 24–26

78. Tsur EE, Shamir A. 2018. Computer-aided design of resistance micro-fluidic circuits for 3D printing. *Comput. Aided Des.* 98:12–23
79. Russell SJ, Norvig P. 2016. *Artificial Intelligence: A Modern Approach*. Essex, United Kingdom: Pearson Educ.
80. Huebner A, Sharma S, Srisa-Art M, Hollfelder F, Edel JB, Demello AJ. 2008. Microdroplets: a sea of applications? *Lab Chip* 8(8):1244–54
81. Hamidović M, Haselmayr W, Grimmer A, Wille R. 2018. *Towards droplet on demand for microfluidic networks*. Paper presented at 3rd Workshop on Molecular Communications, Ghent, Belgium, April 4–6
82. Zhu P, Wang L. 2017. Passive and active droplet generation with microfluidics: a review. *Lab Chip* 17(1):34–75
83. Lashkaripour A, Rodriguez C, Douglas D. 2018. A reverse predictive model towards design automation of microfluidic droplet generators. Paper presented at 10th International Workshop on Bio-Design Automation, Berkeley, CA, July 31–August 3
84. Grimmer A, Hamidović M, Haselmayr W, Wille R. 2019. Advanced simulation of droplet microfluidics. *ACM J. Emerg. Technol. Comput. Syst.* 15(3):26
85. Glawdel T, Ren CL. 2012. Global network design for robust operation of microfluidic droplet generators with pressure-driven flow. *Microfluid. Nanofluidics* 13(3):469–80
86. Gleichmann N, Malsch D, Horbert P, Henkel T. 2015. Toward microfluidic design automation: a new system simulation toolkit for the in silico evaluation of droplet-based lab-on-a-chip systems. *Microfluid. Nanofluidics* 18(5–6):1095–105
87. Grimmer A, Chen X, Hamidović M, Haselmayr W, Ren CL, Wille R. 2018. Simulation before fabrication: a case study on the utilization of simulators for the design of droplet microfluidic networks. *RSC Adv.* 8(60):34733–42
88. Biral A, Zordan D, Zanella A. 2015. Modeling, simulation and experimentation of droplet-based microfluidic networks. *IEEE Trans. Mol, Biol. Multi-Scale Commun.* 1(2):122–34
89. Bardin D, Martz TD, Sheeran PS, Shih R, Dayton PA, Lee AP. 2011. High-speed, clinical-scale microfluidic generation of stable phase-change droplets for gas embolotherapy. *Lab Chip* 11(23):3990–98
90. Brouzes E, Medkova M, Savenelli N, Marran D, Twardowski M, et al. 2009. Droplet microfluidic technology for single-cell high-throughput screening. *PNAS* 106(34):14195–200
91. Grimmer A, Haselmayr W, Springer A, Wille R. 2017. Design of application-specific architectures for networked labs-on-chips. *IEEE Trans. Comput. Aided Des. Integr. Circuits Syst.* 37(1):193–202
92. Grimmer A, Haselmayr W, Wille R. 2019. Automated dimensioning of networked labs-on-chip. *IEEE Trans. Comput. Aided Des. Integr. Circuits Syst.* 38(7):1216–25
93. Grimmer A, Haselmayr W, Wille R. 2020. Automatic droplet sequence generation for microfluidic networks with passive droplet routing. *IEEE Trans. Comput. Aided Des. Integr. Circuits Syst.* 39(2):387–96
94. Martinez AW, Phillips ST, Whitesides GM, Carrilho E. 2010. Diagnostics for the developing world: microfluidic paper-based analytical devices. *Anal. Chem.* 82(1):3–10
95. Fu E, Ramsey SA, Kauffman P, Lutz B, Yager P. 2011. Transport in two-dimensional paper networks. *Microfluid. Nanofluidics* 10(1):29–35
96. Elizalde E, Urteaga R, Berli CL. 2015. Rational design of capillary-driven flows for paper-based microfluidics. *Lab Chip* 15(10):2173–80
97. Nguyen MP, Meredith NA, Kelly SP, Henry CS. 2018. Design considerations for reducing sample loss in microfluidic paper-based analytical devices. *Anal. Chim. Acta* 1017:20–25
98. Potter J, Grover W, Brisk P. 2017. *Design automation for paper microfluidics with passive flow substrates*. Paper presented at Great Lakes ACM Symposium on VLSI, Banff, Alberta, May 10–12
99. DeChiara NS, Wilson DJ, Mace CR. 2017. An open software platform for the automated design of paper-based microfluidic devices. *Sci. Rep.* 7(1):16224
100. Martinez AW, Phillips ST, Whitesides GM. 2008. Three-dimensional microfluidic devices fabricated in layered paper and tape. *PNAS* 105(50):19606–11
101. Liu H, Crooks RM. 2011. Three-dimensional paper microfluidic devices assembled using the principles of origami. *J. Am. Chem. Soc.* 133(44):17564–66

102. Mitani J, Suzuki H. 2004. *Computer aided design for origamic architecture models with polygonal representation*. Paper presented at Computer Graphics International, Crete, Greece, June 19
103. Whitesides G. 2018. Microfluidics in late adolescence. arXiv 1802.05595v1 [physics.flu-dyn]
104. Ababei C, Feng Y, Goplen B, Mogal H, Zhang T, et al. 2005. Placement and routing in 3D integrated circuits. *IEEE Des. Test Comput.* 22(6):520–31
105. Ho W, Ji P. 2006. *Optimal Production Planning for PCB Assembly*. London: Springer
106. Jones DL. 2004. PCB design tutorial, Rev. A. *Electronics.AlternateZone.com*. **http://alternatezone.com/electronics/pcbdesign.htm**
107. Sackmann EK, Fulton AL, Beebe DJ. 2014. The present and future role of microfluidics in biomedical research. *Nature* 507(7491):181–89
108. Moschou D, Tserepi A. 2017. The lab-on-PCB approach: tackling the μTAS commercial upscaling bottleneck. *Lab Chip* 17(8):1388–405
109. Hárendarčíková L, Petr J. 2018. Smartphones & microfluidics: marriage for the future. *Electrophoresis* 39(11):1319–28
110. Hwang Y, Paydar OH, Candler RN. 2015. 3D printed molds for non-planar PDMS microfluidic channels. *Sens. Actuators A* 226:137–42
111. Sochol RD, Sweet E, Glick CC, Wu S-Y, Yang C, et al. 2018. 3D printed microfluidics and microelectronics. *Microelectron. Eng.* 189:52–68
112. Xi W, Kong F, Yeo JC, Yu L, Sonam S, et al. 2017. Soft tubular microfluidics for 2D and 3D applications. *PNAS* 114(40):10590–95
113. Lee JW, Daly SR, Huang-Saad AY, Seifert CM, Lutz J. 2018. Using design strategies from microfluidic device patents to support idea generation. *Microfluid. Nanofluidics* 22(7):70. **https://doi.org/10.1007/s10404-018-2089-6**
114. Lee S, Yan J. 2016. The impact of 3D CAD interfaces on user ideation: a comparative analysis using SketchUp and Silhouette Modeler. *Des. Stud.* 44:52–73
115. Ekströmer P, Wever R. 2019. "Ah, I see what you didn't mean": exploring Computer Aided Design tools for design ideation. *Des. J.* 22(1):1883–97
116. Robertson BF, Radcliffe DF. 2009. Impact of CAD tools on creative problem solving in engineering design. *Comput. Aided Des.* 41(3):136–46
117. Renner G, Ekárt A. 2003. Genetic algorithms in computer aided design. *Comput. Aided Des.* 35(8):709–26
118. Miller JF, Job D, Vassilev VK. 2000. Principles in the evolutionary design of digital circuits—Part I. *Genet. Program. Evolvable Mach.* 1(1–2):7–35
119. Beerel PA, Pedram M. 2018. *Opportunities for machine learning in electronic design automation*. Paper presented at IEEE International Symposium on Circuits and Systems (ISCAS), Florence, Italy, May 27–30
120. Rao RV, Savsani VJ, Vakharia DP. 2011. Teaching–learning-based optimization: a novel method for constrained mechanical design optimization problems. *Comput. Aided Des.* 43(3):303–15
121. Xu H, Liu R, Choudhary A, Chen W. 2015. A machine learning-based design representation method for designing heterogeneous microstructures. *J. Mech. Des.* 137(5):051403
122. Lore KG, Stoecklein D, Davies M, Ganapathysubramanian B, Sarkar S. 2015. Hierarchical feature extraction for efficient design of microfluidic flow patterns. *Proc. Mach. Learn. Res.* 44(1):213–25
123. Lashkaripour A, Rodriguez C, Mehdipour N, McIntyre D, Densmore D. 2019. *Modular microfluidic design automation using machine learning*. Paper presented at *11th International Workshop on Bio-Design Automation (IWBDA-19)*, Cambridge, United Kingdom
124. Wu D, Rosen DW, Wang L, Schaefer D. 2015. Cloud-based design and manufacturing: a new paradigm in digital manufacturing and design innovation. *Comput. Aided Des.* 59:1–14
125. Junk S, Spannbauer D. 2018. *Use of cloud-based computer aided design software in design education*. Paper presented at *17th International Conference on Information Technology Based Higher Education and Training*. Olhao, Portugal, April 26–28
126. Andreadis G, Fourtounis G, Bouzakis K-D. 2015. Collaborative design in the era of cloud computing. *Adv. Eng. Softw.* 81:66–72
127. Wu D, Terpenny J, Schaefer D. 2017. Digital design and manufacturing on the cloud: a review of software and services. *AI EDAM* 31(1):104–18